Identification of Novel Regulators of Mitochondrial Protein Quality Control

Master Thesis

My Bratbakken Lundvall

August 2015

The names of the proteins studied in this project have been censored with respect to ongoing research in The Pon Lab of Columbia University Medical Center.

Supervisor
Professor Liza A. Pon
Department of Pathology and Cell Biology
Columbia University

Examiner
Professor Leif Bülow
Department of Pure and Applied Biochemistry
Lund University

Table of Contents

1. Abstract

Chronic pesticide exposure has been linked to several human diseases including cancer, Parkinson's disease, Alzheimer's disease, multiple sclerosis, cardiovascular disease, and kidney disease. Due to the potential risks to human health, the usage of pesticides has been a controversial topic. Paraquat (PQ), a commonly used pesticide worldwide, has toxic effects due to its generation of reactive oxygen species (ROS) in mitochondria and other cellular compartments. Mitochondria are an essential organelle in eukaryotic cells responsible for energy production, and thus it is intuitive that there exists a dedicated stress response pathway to protect their function. This study focuses on the mitochondria-associated degradation (MAD) pathway, which promotes mitochondrial protein quality control through identification, retrotranslocation, ubiquitination, and degradation of damaged, dysfunctional mitochondrial proteins. We have identified two novel proteins, Y and Z, in MAD, potentially as E3 ubiquitin ligases.

2. List of Abbreviations

BLASTp – Basic Local Alignment Search Tool protein

DUB – Deubiquitinating enzyme

ERAD – Endoplasmic reticulum-associated degradation

MAD – Mitochondria-associated degradation

Mito-roGFP1 – Mitochondria-targeted redox-sensitive Green Fluorescent Protein 1

NCBI – National Center for Biotechnology Information

OD – Optical density

PQ – Paraquat

ROS – Reactive Oxygen Species

UPS – Ubiquitin-proteasome system

WT – Wild-type

3. Introduction

The names and sequences of the proteins studied in this project have been censored with respect to ongoing research in The Pon Lab of Columbia University Medical Center. The actual names have been replaced with the letters X, Y and Z.

The usage of pesticides, also known as insecticides, herbicides, or fungicides, has been a controversial topic for decades due to the potential risks to human health. While pesticides aid in agricultural yield due to the elimination of damaging pests, their extensive use can result in occupational and/or environmental exposure leading to detrimental effects to health. Chronic pesticide exposure has been linked to several human diseases including cancer, Parkinson's disease, Alzheimer's disease, multiple sclerosis, cardiovascular disease, and kidney disease [1-6].

Paraquat (PQ) is a commonly used pesticide worldwide, intended for weed control in both agricultural plantations and public spaces and is registered for use in over 90 countries for many crops, including rice, corn, apples, and sugarcane. Despite its rampant use, in-depth studies analyzing damaging effects of long-term PQ exposure is lacking. Moreover, PQ is classified as highly toxic when inhaled, moderately toxic when ingested and slightly toxic by dermal absorption by the American Environmental Protection Agency (EPA). In plants, PQ functions by shuttling electrons from photosystem I to oxygen, generating the damaging reactive oxygen species (ROS) superoxide [7, 8]. In mammals, PQ cytotoxicity occurs due to the production of ROS within the mitochondria and other cellular compartments upon reduction by NADPH dehydrogenases (Figure 1) [9-13]. Further, exposure to PQ results in lung damage, kidney failure, and heart failure [1] and is linked to chronic diseases, such as Parkinson's disease [2-4].

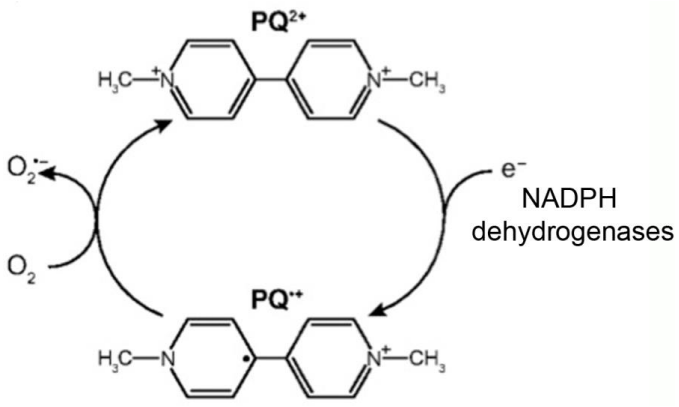

Figure 1. The Redox Cycling Mechanism of Paraquat.
The paraquat dication (PQ^{2+}) undergoes single electron reduction (by NADPH dehydrogenase in yeast) to form the monocation radical ($PQ^{\bullet+}$), which rapidly reacts with oxygen (O_2) to produce superoxide ($O_2^{\bullet-}$) and regenerate the dication (PQ^{2+}) in the mitochondrial matrix. Figure from [13].

In this study, we aim to study cellular response to the widely used pesticide, PQ, using the budding yeast model, *Saccharomyces cerevisiae*. Specifically, we will study the effects of PQ-induced oxidative stress on cellular fitness and viability. *S. cerevisiae* are a great model organism for investigating the role of long-term PQ exposure due to their simple and fast growth. In addition,

budding yeast are easy to manipulate genetically, but have many similarities in the cellular organization and biochemical processes employed in higher eukaryotes. Our study expands our understanding of the mechanisms of cellular quality control activated under conditions of chronic exposure to PQ, which may lead to development of preventative treatment for diseases related to PQ-exposure and oxidative stress to mitochondria.

3.1. Regulation of Mitochondrial Quality Control

Mitochondria are essential organelles in eukaryotic cells critical for cell survival and proliferation. They play a central role in energy production, metabolism, and regulation of apoptosis and calcium signaling. The mitochondrion consists of two phospholipid bilayer membranes, and the inner mitochondrial membrane serves as the site for oxidative phosphorylation, where the electron transport chain shuttles electrons to produce a proton gradient necessary for ATP synthesis [14]. As a central hub for multiple mechanisms, it is not surprising that there exists dedicated pathways to promote mitochondrial quality.

There are two primary levels of control in maintenance of mitochondrial quality: repair mechanisms to reverse damage and elimination mechanisms to remove mitochondria that are beyond repair. Several mechanisms exist to repair mitochondria including, but not limited to interorganelle complementation via mitochondrial fusion, degradation of damaged proteins through the proteases and the ubiquitin proteasome system (UPS), and activation of the mitochondrial unfolded protein response (UPR), to repair and reverse any damage resulting from stress [15-18]. For mitochondrial compartments that are damaged beyond repair, mitochondrial fission sequesters damage to a single compartment, which is targeted for degradation through mitophagy [19]. In mammals, Pink1 and Parkin regulate mitophagy-mediated removal of damaged mitochondria, and loss of function of these players result in chronic diseases, such as Parkinson's disease [20].

As a membrane-bound organelle, mitochondria are not synthesized de novo, but rather are inherited by dividing cells. During yeast cell division, mitochondria line along polarized actin cables and undergo actin cable-dependent movement to the bud tip, where they are anchored to promote their inheritance into the newly forming daughter cell [21]. This is a heavily regulated process, such that the daughter cell inherits fitter mitochondria to ensure production of high functioning daughter cells [22]. This segregation of fit from less fit mitochondria is mediated by the actin cytoskeleton, and serves as a significant quality control mechanism, such that damaged, dysfunctional mitochondria can be sequestered into mother cells to prevent passage into future generations.

3.2. Mitochondria-Associated Degradation (MAD) Mediates Protein Quality Control in the Organelle

Due to its many essential functions, it is intuitive that there exists multiple quality control mechanisms to preserve mitochondrial quality and function. However, mitochondria are the primary site of ROS production through oxidative phosphorylation and thus have the highest exposure to ROS and subsequent oxidative damage compared to other cellular components, and it is not a surprise that cells have adapted a mechanism to protect the organelle from oxidative damage. Mitochondria-associated degradation (MAD) mediates the removal and degradation of damaged mitochondrial proteins by targeting them to the proteasome. This pathway is homologous to the well-characterized ER-associated degradation (ERAD) pathway, where proteins are identified, retrotranslocated to the surface of the organelle, ubiquitinated, and targeted for degradation by the proteasome [23, 24]. While the molecular players involved in MAD are not well characterized, ERAD serves as a foundation to model MAD.

The ubiquitin-proteasome system mediates degradation of damaged proteins through a step-wise process mediated by the collective action of several proteins, including E1, E2, and E3 ubiquitin ligases, which conjugate proteins with ubiquitin at specific lysine residues. E1 activates ubiquitin, which is shuttled to the protein substrate from E2 through the target-specific action of E3 ubiquitin ligases. Generally, proteins contain a minimum of 4 ubiquitin molecules as for targeting to the proteasome for degradation. After polyubiquitination, the protein is extracted from the organelle to the cytosol, where it is presented to the proteasome through the action of Cdc48p (Figure 2). Deubiquitinating proteins (DUB) removes ubiquitin from substrates prior to degradation by the proteasome.

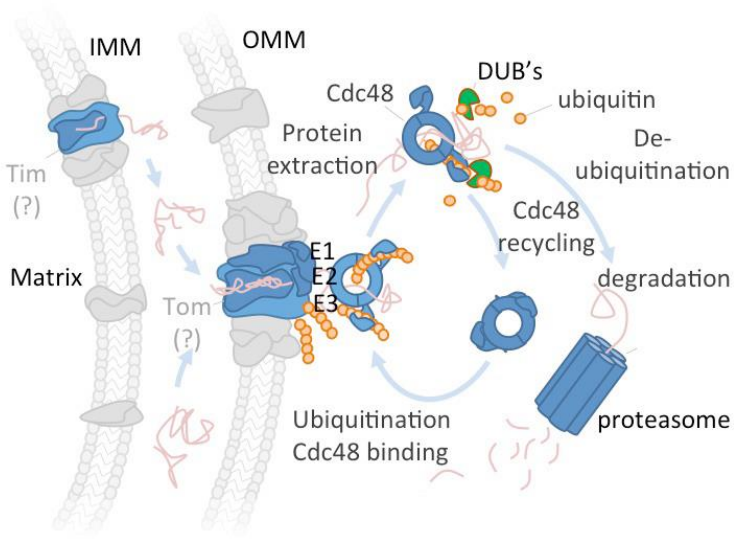

Figure 2. The MAD pathway. Damaged mitochondrial proteins (red) are retrotransported across one or both mitochondrial membranes (IMM and OMM) to the surface of the organelle where they are polyubiquitinated by a cascade of E1, E2 and E3 proteins. The Cdc48p-containing segregase complex extracts polyubiquitinated proteins from the organelle and presents them to the proteasome. DUBs (deubiquitinating proteins) remove ubiquitin from substrates prior to their degradation by the proteasome. Artwork by Wolfgang Pernice of the Pon Lab.

Here we aim to identify the molecular players that mediate the complex series of events in MAD. Specifically, we will study the contribution of the putative E3 ubiquitin ligases, X, Y, and Z (Supplemental table 1) in MAD using *S. cerevisiae* as a model system. Transcriptome analysis revealed that the genes *X*, *Y, and Z* were massively upregulated during conditions of chronic exposure to mild, PQ-induced oxidative stress. Previous reports have identified that X localizes to mitochondria, has E3 ubiquitin ligase activity in vitro, and can bind to Cdc48p [25-28]. Y and Z both bind to the E3 scaffold protein, Cdc53p [29], and contains putative F-box motifs [30]. Furthermore, the outer mitochondrial membrane protein Y ubiquitinates an integral mitochondrial membrane protein required for mitochondrial fusion [31, 32] and deletion of *Y* affects mitochondrial morphology and distribution [33].

4. Materials and methods

4.1 Yeast Growth Conditions

The *S. cerevisiae* strain BY4741 (*MATa his3Δ1 leu2Δ0 met15Δ0 ura3Δ0*) from Open Biosystems (Huntsville, AL) was used to construct all recombinant strains (Supplemental table 2). Standard rich medium (YPD) was used for growth of strains, unless otherwise indicated. For strains where dropout medium was required, synthetic complete (SC) medium with the essential amino acid dropouts was used. Non-fermentable glycerol-based medium (YPG) was used for studies requiring selection for respiration-competence. Cells were grown in 5 mL of liquid medium in 50-mL conical-bottom tubes at 30°C in a shaking incubator. All experiments were carried out with cultures grown to mid-log phase in liquid medium (OD_{600} = 0.1 - 0.3).

4.2 Strain Construction

All strains used in this study (Supplemental table 2) were manipulated in wild-type BY4741 cells. Deletion strains were constructed by replacing the gene of interest at the chromosomal locus with an auxotrophic marker (e.g. *LEU2*) using PCR-based recombination. Specifically, PCR products containing the coding sequence of *LEU2* and sequences directly upstream of the start codon and downstream of the stop codon of the gene of interest were amplified from the plasmid POM13 (Addgene, Cambridge, MA) using primers listed in Supplemental table 3. Cells were transformed with the PCR product using a standard lithium acetate protocol [34] and selected for on SC medium with appropriate dropouts. Transformants were screened via PCR using primers listed in (Supplemental table 3).

MLY016 was constructed by replacing the *Z* gene at the chromosomal locus in strain MLY004 using the method described above with the selection marker *kanMX6,* providing resistance to geniticin. mito-roGFP1 was expressed in cells through a plasmid harboring the mito-roGFP1 under a constitutively active GPD promoter.

4.3 Measurement of Growth Rates

BY4741, *X*Δ, *Y*Δ, *Z*Δ and *Y*Δ*Z*Δ cells were grown to mid-log phase in YPD, diluted to OD_{600} = 0.0035 and grown in YPD with and without 2.5 mM PQ in a sterile 96-well plate. OD_{600} measurements were taken every 20 minutes for 220 cycles using a Tecan Nanoquant plate reader (Tecan US, Morrisville, NC) to determine maximum growth rate and maximum slope during logarithmic growth. The plate reader was operated using Magellan software.

4.4 Measurement of Growth using Serial Dilutions

Serial dilutions were used to assess growth of mutants on solid media in the presence of oxygen. BY4741, *X*Δ, *Y*Δ, *Z*Δ and *Y*Δ*Z*Δ cells were grown to mid-log phase in YPD and diluted to OD_{600} = 0.01. Serial dilutions were performed on a fermentable, glucose-based carbon source to determine

growth. 10-fold serial dilutions were performed in YPD and 5 µl was placed on solid YPD and grown for 30°C for three days. BY4741, *X*Δ, *Y*Δ, *Z*Δ and *Y*Δ*Z*Δ cells were grown to mid-log phase in YPG and diluted to OD_{600} = 0.01. Serial dilutions were performed on a non-fermentable, glycerol-based carbon source to determine respiration competence and PQ-sensitivity in actively respiring cells. 10-fold serial dilutions were performed in YPG and 5 µl was placed on solid YPG with and without 0.5 mM PQ and grown for 30°C for four days. Plates were imaged using a ChemiDoc MP Imaging system (Bio-Rad, Hercules, CA).

4.5 Measurement of Petite Frequency using Colony Size

BY4741, *X*Δ, *Y*Δ, *Z*Δ and *Y*Δ*Z*Δ cells were grown to mid-log phase in YPG. Approximately 300 cells were plated on solid YPD-GLY (3% glycerol, 0.1% glucose) medium and grown at 30°C for five days. Plates were imaged using a ChemiDoc MP Imaging system (Bio-Rad, Hercules, CA). Colony sizes were quantified by number of pixels per colony using CellProfiler software, and binned according to pixel count as indicated.

4.6 Quantification of Protein Ubiquitination using Western Blotting

For quantification of protein ubiquitination, whole cell extracts were isolated from cells were grown to mid-log in synthetic medium supplemented with proline (0.17% yeast nitrogenous base without ammonium sulfate) supplemented with 0.1% proline, amino acids, and 2% glucose. Cells were incubated with and without 2.5 mM PQ for 12 h followed by incubation with 0.003% SDS for 2 h, followed by incubation with and without PQ and either 75 µM MG132 (Z-Leu-Leu-Leu-al; Sigma, St. Louis, MO) or equal concentration DMSO for an additional 4 h prior to protein collection [35].

Proteins were isolated from yeast cells as previously described [36]. Briefly, cells were collected and lysed by auto-vortexing with 0.5 mm glass beads and lysis buffer (10 % glycerol, 10 mM EGTA, 1 % Triton X-100, 50 mM Tris-HCl pH 7.5, 150 mM NaCl, 2 mM PMSF, and protease inhibitor cocktail). The samples were centrifuged and the protein lysate was collected and immediately frozen on dry ice and stored at -80 °C. Protein concentrations were determined with the BCA assay using vendor's protocol (Pierce, Rockford, IL).

Proteins were separated based on size on a 10% SDS-polyacrylamide gel, transferred onto a PVDF membrane and immunoblotted with mouse monoclonal anti-Ubiquitin antibody (MAB1510, Millipore, Temecula, CA). Secondary antibody conjugated to horseradish peroxidase was used for visualization of the protein using Luminata Forte Western Blot HRP substrate (Millipore, Temecula, CA). In-gel trichloroethanol-staining was used as a load control [37]. All gel and blot imaging was performed using a ChemiDoc MP imaging system and analyzed using Image Lab software (Bio-Rad, Hercules, CA).

4.7 Microscopy

For visualization of mitochondria and mitochondrial DNA, wild-type BY4741, *X*Δ, *Y*Δ, *Z*Δ, and *Y*Δ*Z*Δ cells expressing C-terminally GFP-tagged Cit1p were grown in SC at 30°C. Mid-log phase cells were stained with 0.5 µg/ml DAPI suspended in mounting solution. Stained cells were mounted on microscope slides and imaged using an Axioskop 2 microscope equipped with 100x/1.4 Plan-Apochromat objective (Zeiss, Thornwood, NY) and an Orca 1 cooled CCD camera (Hamamatsu). DAPI and GFP fluorophores were excited by a mercury arc lamp and imaged through a motorized filter wheel using the following filters: DAPI (excitation 402/15, emission 455/50), GFP (excitation 482/28, emission 525/50). Hardware was controlled by Nikon Elements software. Z-series were collected through the entire cell at 0.5-µm intervals using 1x1 binning and 25 ms exposure time for DAPI and 100 ms exposure time for GFP. Images were deconvolved using a constrained iterative restoration algorithm with the following parameters: 460 nm emission wavelength for DAPI or 507 nm emission wavelength for GFP, 30 iterations, 100% confidence limit.

Measurement of redox state were performed using mito-roGFP1 as previously described [38]. Briefly strains expressing mito-roGFP1 were grown to mid-log phase and 1.5 µl of concentrated cell suspension was applied to a microscope slide, covered with a cover slip, and imaged immediately. mito-roGFP1 was imaged on a Zeiss AxioObserver.Z1 microscope (Carl Zeiss Inc., Thornwood, NY) equipped with a metal halide lamp, modified GFP filter (Zeiss filter set 46 HE with excitation filter removed, dichroic FT 515, emission 635/30) and an Orca ER cooled CCD camera (Hamamatsu Photonics, Bridgewater, NJ) and driven by Axiovision software (Carl Zeiss Inc., Thornwood, NY). Z-series were collected through the entire cell at 0.5 µm intervals using 1x1 binning, 365 nm LED at 25% power with 100 ms exposure time for oxidized form and 470 nm LED at 100% power with 100 ms exposure time for reduced form, with analog gain at 216. Images were deconvolved using a constrained iterative restoration algorithm with the following parameters: 507 nm excitation wavelength, 30 iterations over 100% confidence. For quantification of redox state, Volocity software with background selection and thresholding steps was used.

4.8 Statistical Methods

All statistical analysis, construction of notched dot box plots, and determination of p-values were done using the Microsoft Excel add-on Analyze-it. Non-parametric analysis was applied for all data using the Kruskal-Wallis test to determine p-values for all data sets.

4.9 Analysis of Sequence Homology using BLASTp

The protein sequences of Y and Z (Supplemental table 1) were analyzed for sequence homology with *Homo sapiens* using the Basic Local Alignment Search Tool (BLASTp) of the National Center for Biotechnology Information (NCBI).

5. Results & Discussion

5.1 Deletion of Putative E3 Ub Ligases Results in Growth-inhibiting Effects of PQ

Under conditions of stress, cells mount adaptive response mechanisms to mitigate potential damage to cellular structures including organelles, proteins, and lipids. Indeed, several studies have identified novel mechanisms in protection of mitochondrial integrity under conditions of stress [16, 39]. Previous studies in the lab used transcriptome analysis on PQ-treated yeast cells to identify novel mechanisms involved in maintenance of mitochondrial quality under chronic oxidative stress. These studies revealed pathways involved in protein quality control directed at restoring mitochondrial fitness and function. Specifically, they identified several putative E3 ubiquitin ligases, believed to play a role in ubiquitin-mediated targeting of mitochondrial proteins for degradation by the ubiquitin-proteasome system (UPS): *X*, *Y*, *Z* [26, 27, 29, 30, 40].

To investigate the importance of these proteins for the adaptive response under conditions of oxidative stress, we tested the effect of the deletion of *X, Y,* and *Z* under mild, chronic PQ exposure. We find that PQ exposure has a growth-inhibiting effect in wild-type, *X*Δ, *Y*Δ and *Z*Δ cells (Figure 3). Y and Z are both putative E3 ubiquitin ligases, which may potentially have redundant functions. Therefore, we tested the effect of simultaneous deletion of both *Y* and *Z* on the growth-inhibiting effects of PQ exposure. Surprisingly, we only find a minor decrease in sensitivity to the growth-inhibiting effects of PQ in *Y*Δ, *Z*Δ and *Y*Δ*Z*Δ cells, but not *X*Δ cells compared to wild-type cells (Figure 3).

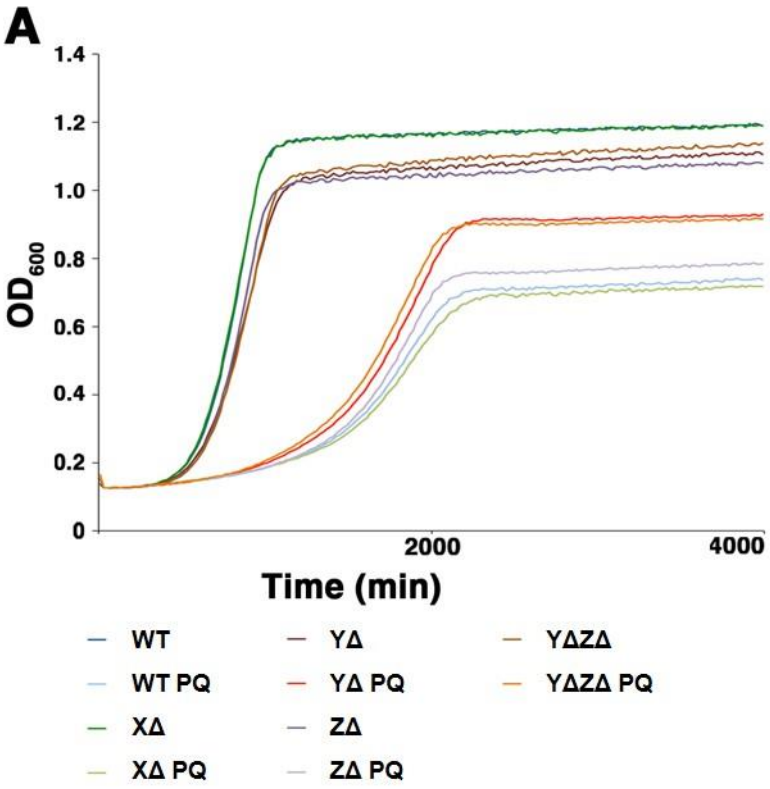

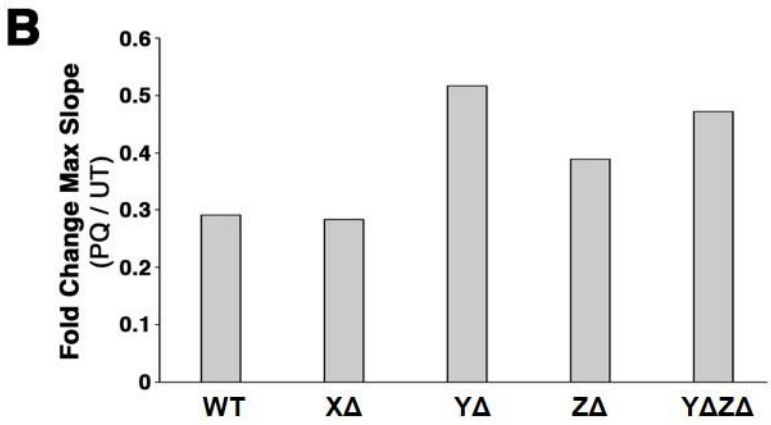

Figure 3. Deletion of putative E3 ubiquitin ligases results in growth-inhibiting effects of PQ.

A) Growth rates of wild-type, *X*Δ, *Y*Δ, *Z*Δ and *Y*Δ*Z*Δ cells were measured in liquid YPD media with and without 2.5 mM PQ. OD_{600} measurements were taken every 20 min and plotted as a function of time. Data is representative of 3 independent trials.

B) Fold changes of the ratio of max growth rates of 2.5 mM PQ-treated versus untreated wild-type, *X*Δ, *Y*Δ, *Z*Δ and *Y*Δ*Z*Δ cells.

Yeast cells can exploit either fermentation or respiration for energy production. During growth on glucose (a fermentable carbon source), yeast cells can undergo fermentative growth and do not require functional mitochondrial respiration. Furthermore, growth on glucose results in repression of mitochondrial biogenesis [41]. Therefore, growth rates on glucose may not be the most sensitive method to assess mitochondrial function and sensitivity to PQ. For that reason, we studied the effects of deletions of putative regulators of mitochondrial quality and of PQ treatment on the growth rates of cells using the non-fermentable carbon source glycerol. Under growth in glycerol, yeast cells must utilize oxidative respiration, and thus are dependent on fully functional mitochondria.

As expected, we find that *X*Δ, *Y*Δ, *Z*Δ and *Y*Δ*Z*Δ cells grow similar to wild-type cells on glucose (Figure 4A). However, cells carrying *Y* deletion grow slower compared to wild-type, *X*Δ and *Z*Δ cells on glycerol (Figure 4A-B). Furthermore, we find that *Y*Δ and *Y*Δ*Z*Δ cells display increased sensitivity to PQ when grown on glycerol (Figure 4B). These data suggest that Y is important for the maintenance of mitochondrial function and response to PQ-induced oxidative stress.

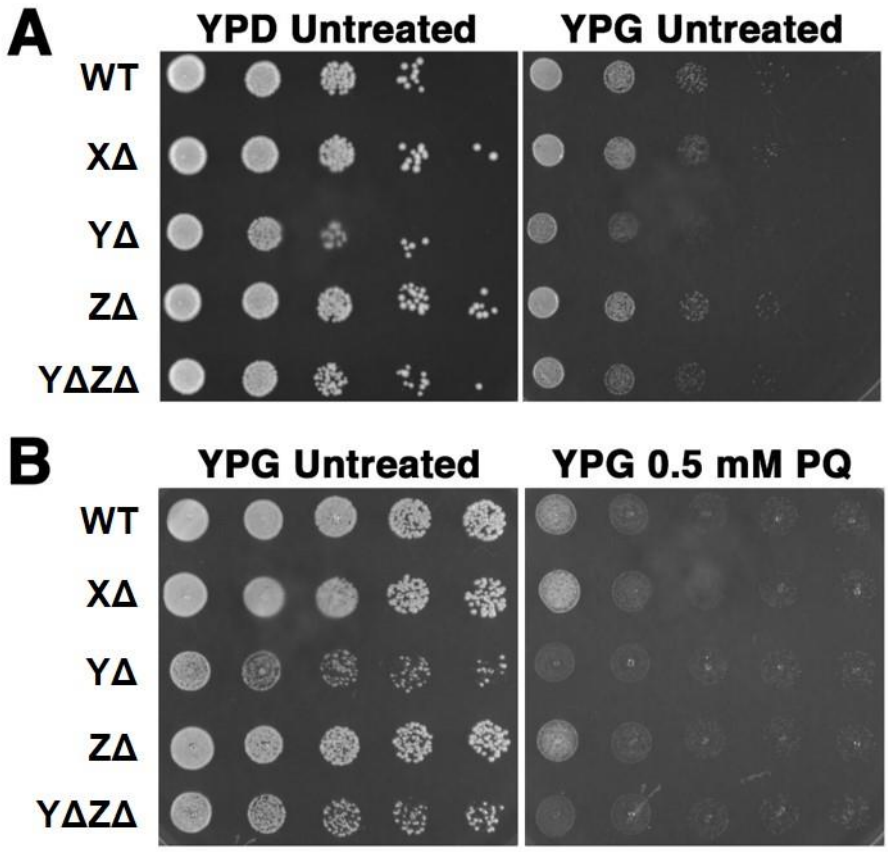

Figure 4. *Y*Δ cells exhibit decreased mitochondrial function and increased sensitivity to PQ. A) BY4741, *X*Δ, *Y*Δ, *Z*Δ and *Y*Δ*Z*Δ cells were grown to mid-log phase in YPD and diluted to OD_{600} = 0.01. 10-fold serial dilutions were performed in YPD and 5 µl was placed on solid YPD and YPG and grown at 30°C for three days. Plates were imaged on a Bio-Rad ChemiDoc MP Imaging system. Images are representative of 3 independent trials. B) BY4741, *X*Δ, *Y*Δ, *Z*Δ and *Y*Δ*Z*Δ cells were grown to mid-log phase in YPG and diluted to OD_{600} = 0.01. 10-fold serial dilutions were performed in YPG and 5 µl was placed on solid YPG with and without 0.5 mM PQ and grown at 30°C for four days. Plates were imaged on a Bio-Rad ChemiDoc MP Imaging system. Images are representative of 3 independent trials.

5.2 The Defects in Mitochondrial Function in *YΔ* Cells is Not Due to Loss of mtDNA

Since cells carrying a *Y* deletion display impaired mitochondrial function, we investigated whether the defects were due to loss of mitochondrial DNA (mtDNA). mtDNA encodes genes required for respiration, and since yeast cells can exploit either fermentation or respiration for energy production, they can grow in spite of lost or mutation of mtDNA on glucose-rich medium. Cells that contain wild-type mtDNA (*rho*$^{+}$ cells) are respiration-competent, but *rho*^{0} cells (which have no mtDNA) and *rho*$^{-}$ cells (which carry mutations in mtDNA) are respiration incompetent. Commonly, petite frequency – frequency of small colony formation – is used to determine defects in mtDNA maintenance. More specifically, *rho*^{0} cells or *rho*$^{-}$ cells form smaller colonies than *rho*$^{+}$ cells when grown on a non-fermentable carbon source supplemented with low levels of glucose (YPD-GLY – 3% glycerol, 0.1% glucose), due to their inability to respire and utilize glycerol as an energy source [42, 43].

Here, we measured relative colony size of cells grown on YPD-GLY plates for 5 days using CellProfiler as described in *Section 4. Materials and Methods*. We find that deletion of *Y* results in increased petite frequency both in wild-type and *ZΔ* cells, while deletion of *Z* alone does not affect petite frequency (Figure 5A). However, the petite frequency is not as high as those found in cells bearing a deletion in genes required for maintenance of mtDNA (e.g. *mgm101Δ* cells) (data not shown). These data confirm that Y, but not Z plays a role in maintenance of mitochondrial function, resulting in mixed populations of *rho*$^{+}$ and *rho*^{0} or *rho*$^{-}$ cells when grown on glucose-based carbon sources. Moreover, *YΔ* and *YΔZΔ* cells have a higher petite frequency than wild-type cells and *XΔ* cells (Figure 5A).

Unfortunately it is not possible to distinguish between populations of *rho*^{0} and *rho*$^{-}$ cells using petite frequency. Therefore, we used the DNA-binding dye, DAPI to visualize mtDNA in wild-type *XΔ*, *YΔ*, *ZΔ* and *YΔZΔ* cells. As mtDNA localize as punctate nucleoid structures within mitochondria, *rho*^{0} cells are distinguishable due to their lack of punctate structures.

We find that all wild-type and *ZΔ* cells contain mtDNA (Figure 5B). We also find that a very small amount (< 3.4%) of *XΔ*, *YΔ* and *YΔZΔ* cells lack mtDNA and are thus classified as *rho*^{0} cells (Figure 5B). These data suggest that the impaired mitochondrial function displayed by cells carrying the *Y* deletion is not due to loss of mtDNA. It is possible that the mitochondrial defects are due to respiration-incompetence as a result of mutations in the mtDNA (*rho*$^{-}$cells), or due to disruptions of protein structures or critical mitochondrial maintenance pathways.

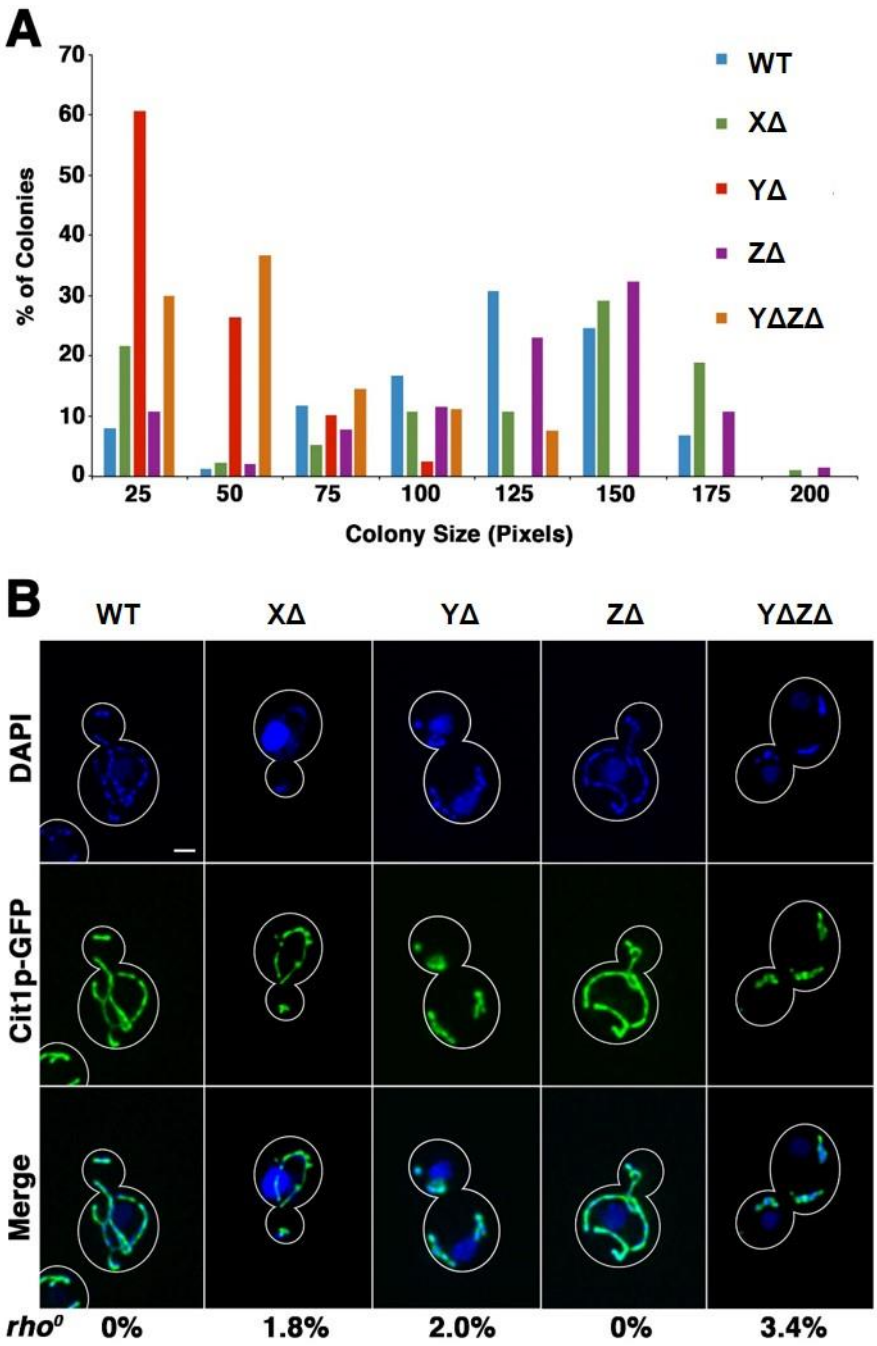

Figure 5. Yp plays a role in maintenance of mitochondrial DNA.

A) BY4741, *X*Δ, *Y*Δ, *Z*Δ and *Y*Δ*Z*Δ cells were grown to mid-log in YPG. ~300 cells were plated on solid YPD-GLY (3% glycerol, 0.1% glucose) medium and grown for 5 days at 30°C. Plates were imaged on a Bio-Rad ChemiDoc MP Imaging system. Colony sizes were quantified by number of pixels per colony using CellProfiler software. Data is representative of 2 independent trials. B) DAPI staining was used to visualize mtDNA in mitochondria in BY4741, *X*Δ, *Y*Δ, *Z*Δ and *Y*Δ*Z*Δ cells expressing Cit1p-GFP. Cell were grown in SC, mid-log phase cells were treated with 0.5 µg/ml DAPI for 15 min. Wide-field z-series were collected through the entire cell at 0.5 µm intervals and deconvolved using a constrained iterative restoration algorithm with the following parameters: 460 nm emission wavelength for DAPI, 507 nm emission wavelength for GFP, 30 iterations, 100% confidence limit. Cell outlines were drawn over phase images. Images are representative of one trial. Scale bar, 1 µm. *Rho*^{0} percentage equals the fraction of budding cells carrying no mtDNA.

5.3 Deletion of *Y* Results in Decreased Overall Mitochondrial Redox-fitness

Determining differences in growth is a good indication of mitochondrial function. However, growth does not provide a direct measurement of mitochondrial quality. Previous work from the lab has demonstrated that mitochondrial redox-state decreases both under conditions of stress and as a function of age [22, 44], and thus serves as a good indicator of mitochondrial fitness. Specifically, younger and healthier cells have more reduced mitochondria. Here we measured mitochondrial redox-state using roGFP1 targeted to the mitochondrial matrix, renamed mito-roGFP1 [38]. Briefly, mito-roGFP1 is a ratiometric biosensor in which oxidation of roGFP1 causes a conformational change that shifts its optimal excitation wavelength from ~480 nm to ~400 nm, allowing reliable measurements of relative redox-state [45].

We find that *Y*Δ and *Y*Δ*Z*Δ cells have more oxidized mitochondria compared to wild-type, *X*Δ, and *Z*Δ cells (figure 6). These data are consistent with our previous findings that Y, but not X or Z, function in maintenance of mitochondrial quality. Interestingly we find that *Y*Δ*Z*Δ cells have more reduced mitochondria than *Y*Δ cells, similar to the lower petite frequency of *Y*Δ*Z*Δ cells compared to *Y*Δ cells. These data further supports the idea that the loss of Z induces an adaptive stress response that is somehow protective of mitochondrial function.

We then measured mitochondrial redox-state under PQ-induced oxidative stress. As expected, mitochondria in wild-type, *X*Δ, *Y*Δ, *Z*Δ and *Y*Δ*Z*Δ cells are significantly more oxidized during chronic exposure to low levels of PQ (Figure 6). Moreover, we find that *Y*△ and *Y*Δ*Z*Δ cells exposed to PQ exhibit the highest level of mitochondrial oxidation compared to other strains. These data provide further evidence that Y alone and potentially in conjunction with Z function in maintenance of mitochondrial quality under conditions of PQ-induced mitochondrial damage.

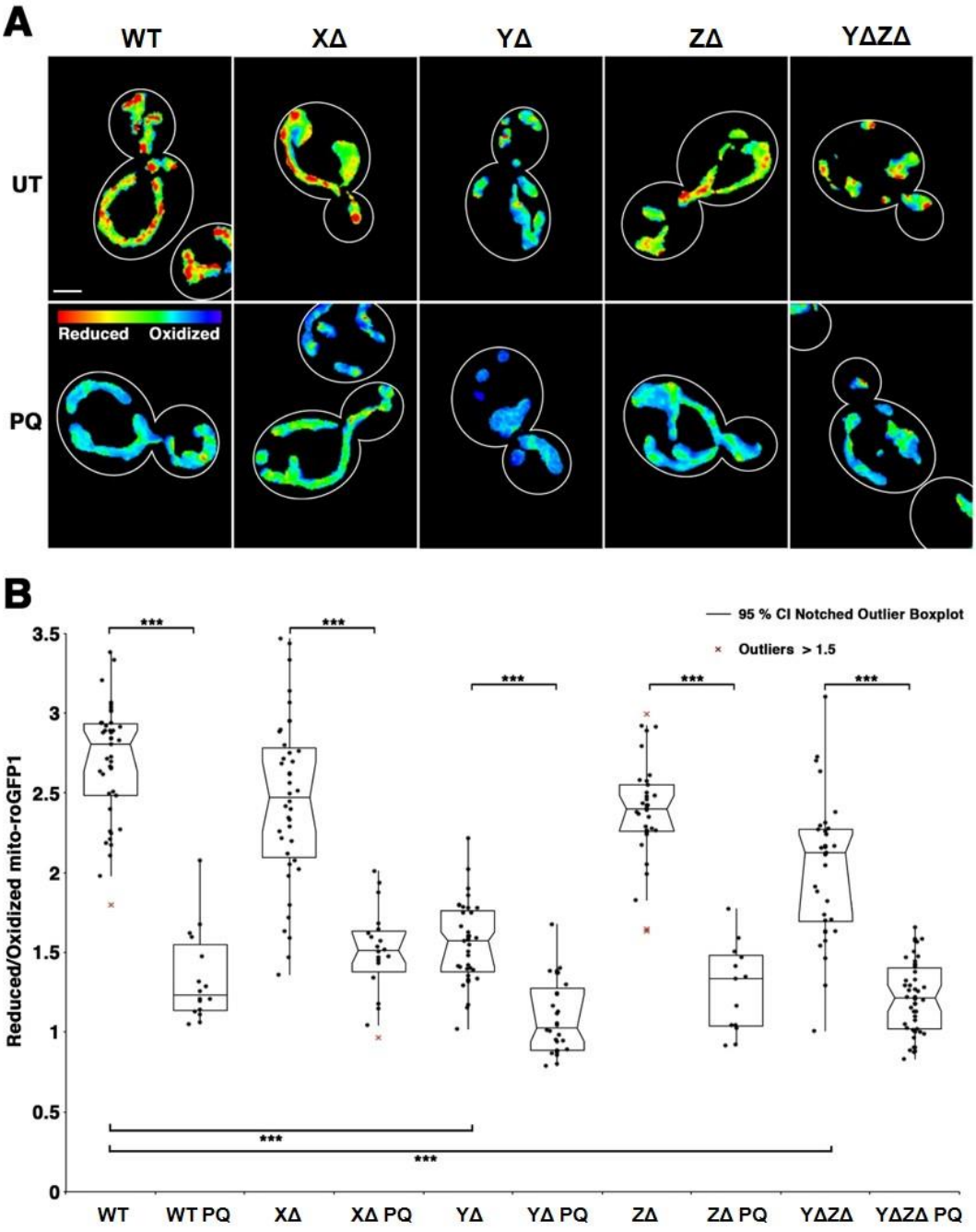

Figure 6. Deletion of *Y* results in decreased overall mitochondrial redox- fitness and decreased sensitivity to PQ-induced oxidative stress.

A) mito-roGFP1 was used to visualize redox-state of mitochondria in BY4741, *X*Δ, *Y*Δ, *Z*Δ and *Y*Δ*Z*Δ cells grown in SC-URA with and without 2.5 mM PQ for 12 h. Wide-field z-series were collected through the entire cell at 0.5 µm intervals and deconvolved using a constrained iterative restoration algorithm with the following parameters: 507 nm emission wavelength, 30 iterations, 100% confidence limit. Images are reduced:oxidized mito-roGFP1 ratios. Color scale indicates ratio values; warmer colors indicate more reduced mitochondria. Cell outlines were drawn over phase images. Images are representative of one trial. Scale bar, 1 µm. B) Notched dot box plot of the average reduced:oxidized mito-roGFP1 ratio in BY4741, *X*Δ, *Y*Δ, *Z*Δ and *Y*Δ*Z*Δ cells. *** = p-value < 0.001 based on non-parametric Kruskal-Wallis testing with pairwise Bonferroni correction. Results are representative of one trial.

5.4 Simultaneous Deletion of *Y* and *Z* Results in Decreased Protein Ubiquitination under PQ-induced Oxidative Stress

We have confirmed that Y plays a significant role in regulation of mitochondrial quality control. Next we aimed to test directly whether Y exerts its function on mitochondrial quality through MAD. Y and Z have previously been predicted to be E3 ubiquitin ligases [29-33], functioning in mitochondrial quality control by polyubiquitinating mitochondrial proteins to target them for degradation by the UPS. Under conditions of oxidative stress, there is an increase in overall cellular damage, such as misfolded and damaged proteins. These proteins are subsequently ubiquitinated for targeting to the proteasome by the concerted effort of E1, E2, and E3 ubiquitin ligases, resulting in an increase in the total cellular ubiquitination. Here, we quantified protein ubiquitination levels by western blotting to determine the effects of *Y* and Z deletion in this process. Ubiquitinated proteins are transported to the proteasome where they are degraded, and thus we performed quantification on cells treated with the proteasome-inhibitor, MG132.

As expected, there is an increase in total ubiquitination levels in wild-type cells under conditions of PQ-induced oxidative stress (figure 7A-B). Surprisingly, we find that *Y*Δ and *Z*Δ cells have increased total ubiquitination levels comparable to wild-type cells, despite their predicted roles as E3 ubiquitin ligases (Figure 7A-B). This may be due to redundant and/or compensatory functions of the two proteins. To test this hypothesis, we quantified the ubiquitination levels of *Y*Δ*Z*Δ cells. Indeed, we find a significant decrease in total ubiquitination levels compared to wild-type, *Y*Δ and *Z*Δ cells (Figure 7A-B). These results are not due to changes in proteasome activity (Figure 7C). These data suggest that both Y and Z mediate the ubiquitination of proteins through similar mechanistic pathways, potentially as E3 ubiquitin ligases and that Y and Z ubiquitination targets the protein for degradation by the proteasome, similar to previously characterized E3 ubiquitin ligases [28, 46].

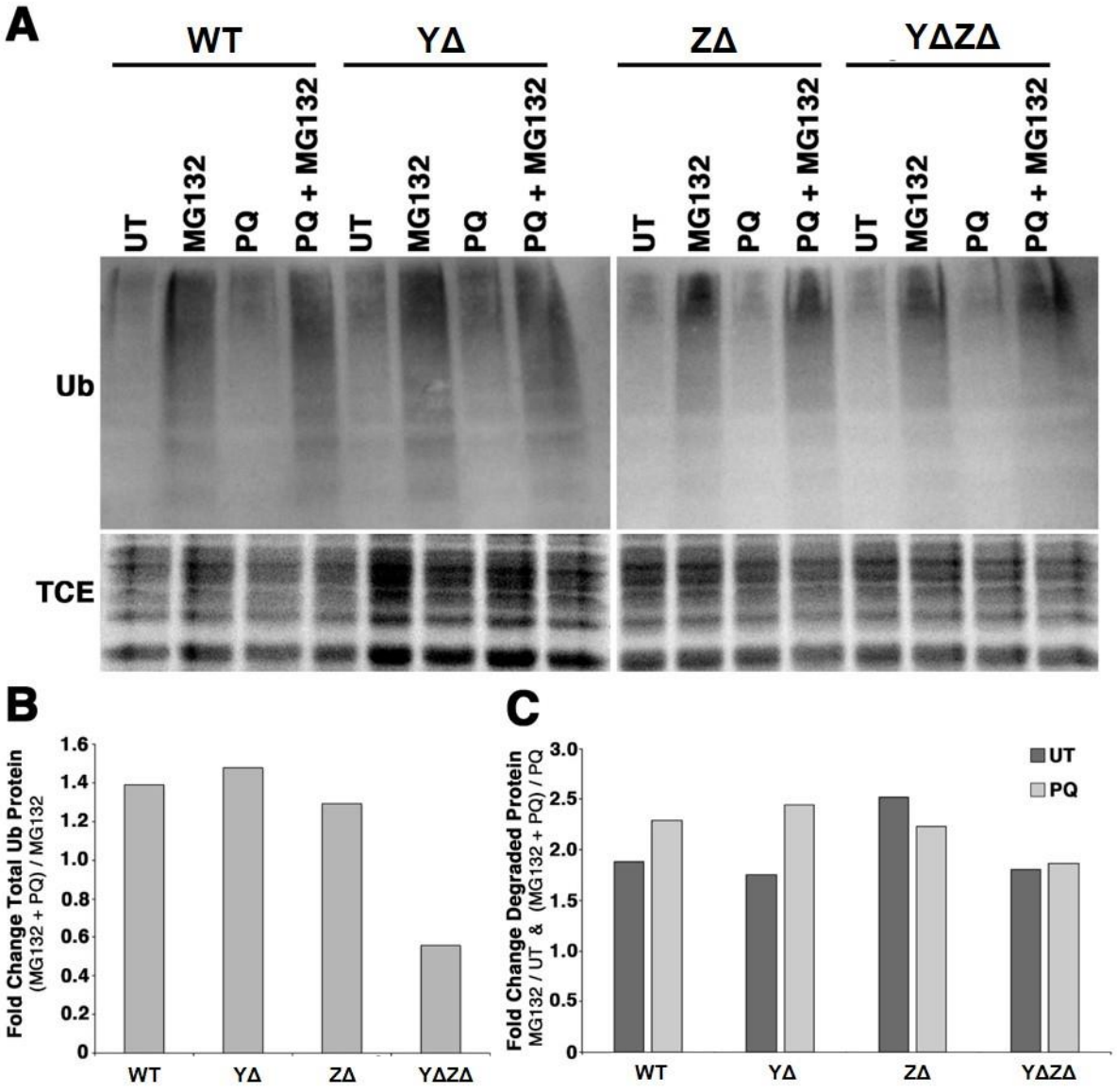

Figure 7. Simultaneous deletion of *Y* and *Z* results in decreased protein ubiquitination under PQ-induced oxidative stress.

Whole cell extracts were collected from BY4741, *Y*Δ, *Z*Δ and *Y*Δ*Z*Δ cells with the indicated treatments (UT = Untreated, MG132 = Proteasome inhibitor, PQ = Paraquat). Cells were incubated with and without 2.5 mM PQ for 12 h followed by incubation with and without PQ and either 75 µM MG132 or equal concentration DMSO for an additional 4 h prior to protein collection. Proteins were separated based on size on a 10% SDS-polyacrylamide gel and transferred to a PVDF membrane for antibody probing. A) Top panel: Membranes were probed with a monoclonal anti-ubiquitin antibody. Bottom panel: In-gel TCE staining of total proteins was used as a loading control. Results are representative of 1 trial. B) Quantification of the fold change of total ubiquitination levels in PQ and MG132 treated cells compared to MG132 treatment alone. C) Quantification of the fold change of MG132 treated versus untreated cells in PQ-treated (light grey) and untreated (dark grey) cells.

5.5 The F-box Motifs of Y and Z are Conserved in *Homo sapiens*

We have shown that both Y and Z mediate the ubiquitination of proteins, potentially as E3 ubiquitin ligases active in MAD. Since PQ has been connected with Parkinson's disease and other complications in humans, we wanted to see whether there exists similar mitochondrial quality control proteins in humans as the ones we have found in yeast.

To determine this we analyzed the protein sequences of Y and Z (Supplemental table 1) using NCBI's BLASTp, searching for alignments with the entire genome of humans, *Homo sapiens.* The BLASTp confirmed the F-box motif of Y, situated within the first 100 amino acids, and recognized 33% identity with the human F-box protein Fbx3. The analysis of Z identified several leucine-rich repeats and recognized 25-33% identity with several human F-box and leucine-rich repeat proteins. These results indicate that the F-box motif is conserved over the species. However, the molecular players of MAD in yeast identified in this study do not seem to be conserved in humans. This however does not rule out the possibility of human E3 Ub ligases with similar functions as Y and Z, and a quality control pathway similar to MAD may exist also in humans.

6. Conclusions

Contrary to controlled laboratory conditions, environments undergo constant change such that organisms have developed adaptive stress response pathways to maintain cellular health. Here, we used the budding yeast model system to study the oxidative stress response dedicated to preserving mitochondrial quality under conditions of stress. Specifically, MAD, the mitochondrial homologue to ERAD [23, 24], protects mitochondrial quality under stress by mediating removal and degradation of damaged proteins within the organelle. We modelled chronic oxidative stress using the pesticide, PQ due to its commercial usage despite high correlation with many chronic diseases including Parkinson's, diabetes, cancer, cardiovascular, and renal dysfunction [1-6]. Our studies have identified Y and Z as two novel players in this mechanistic pathway.

It is intuitive that growth rate correlates with cellular fitness, as healthier cells grow at a faster rate than unhealthy cells. Exposure to damaging agents, such as PQ-induced oxidative stress, results in defects in cellular fitness, ultimately affecting growth rate negatively. Therefore, we used measurements of growth rate under PQ-exposure as an initial screen to confirm the role of the top hits in the transcriptome analysis previously performed in the lab (X, Y, and Z) in the oxidative stress response. The expression of *X*, *Y*, and *Z* all increased significantly under chronic PQ exposure. We found that *X*Δ, *Y*Δ, *Z*Δ and *Y*Δ*Z*Δ cells grow similar to wild-type cells in glucose-based medium, and that *Y*Δ, *Z*Δ and *Y*Δ*Z*Δ are actually more sensitive to the growth-inhibiting effects under conditions of growth using glucose as a carbon source. However, glucose is not an appropriate medium to study mitochondrial fitness, as growth on glucose does not require functional mitochondrial respiration, and causes repression of mitochondrial biogenesis [41]. Consequently, we replaced glucose with the non-fermentable carbon source glycerol to study growth. We found that cells carrying *Y* deletion grow less compared to wild-type, *X*Δ and *Z*Δ cells on glycerol, and that *Y*Δ and *Y*Δ*Z*Δ cells display increased sensitivity to PQ. These findings suggest that Y alone, and potentially together with Z play an important role in the maintenance of mitochondrial function.

Since cells carrying an *Y* deletion have impaired mitochondrial function, we wanted to do a more direct assessment of the respiration-competence of each strain. Respiration-incompetent cells (rho^0/rho^- cells) form smaller colonies than respiration-competent cells (rho^+ cells) when grown on medium containing glycerol and a limited amount of glucose. We found that *Y*Δ and *Y*Δ*Z*Δ cells have increased ratios of respiration-incompetent cells compared to wild-type, *X*Δ and *Z*Δ cells. Cells carrying the single deletion of *Y* have higher petite frequency than cells carrying the double deletion of *Y* and *Z,* suggesting that there may be an adaptive response when Z is absent that is protective of the cell. As respiration-incompetence often correlates with loss of mtDNA, we performed DAPI staining to determine the ratio of cells that contain no mtDNA (rho^0 cells). We found that wild-type, *X*Δ, *Y*Δ, *Z*Δ

and *Y*Δ*Z*Δ cells have no, or very low frequency of *rho*^{0} formation. Therefore, defects in mitochondrial function displayed by cells carrying the *Y* or *Y* and *Z* deletions are not due to loss of mtDNA.

Growth is an energy-demanding process, and thus maintenance of mitochondrial quality is essential for proper growth. Exposure to PQ results in formation of superoxides in compartments including mitochondria, resulting in oxidative damage to the organelle and subsequent decrease in growth rates [8]. Thus we measured mitochondrial fitness in our MAD mutants by measuring mitochondrial redox-state using mito-roGFP1, where more reduced mitochondria are characterized as more fit. As expected, wild-type cells chronically exposed to low levels of PQ show a significant increase in oxidized mitochondria. However, *Y*Δ and *Y*Δ*Z*Δ cells have more oxidized mitochondria overall than wild-type, *X*Δ, and *Z*Δ cells. These data are consistent with previous findings that deletion of *Y* alone and potentially in conjunction with *Z* results in loss of maintenance of mitochondrial quality.

Oxidative stress results in the damage of proteins, DNA, lipids and other cellular components. MAD acts to counteract the oxidative stress by targeting damaged proteins for degradation by the proteasome through a multi-step mechanism: recognition of damaged proteins, translocation to the cytosol, and polyubiquitination by E1, E2 and E3 ubiquitin ligases. Sequence analysis showed that Y and Z have putative E3 ubiquitin ligase domains. Therefore we quantified total protein ubiquitination levels by western blot analysis in wild-type, *Y*Δ, *Z*Δ and *Y*Δ*Z*Δ cells under conditions of PQ-induced oxidative stress. As expected, we find an increase in total ubiquitination levels in wild-type cells after chronic exposure to PQ. We also find that *Y*Δ and *Z*Δ cells have increased total ubiquitination levels comparable to wild-type cells. It is possible that these two proteins have redundant or compensatory functions, and thus we studied the *Y*Δ*Z*Δ double deletion strain. Interestingly, we find decreased levels of ubiquitination in *Y*Δ*Z*Δ cells, which are not due to changes in proteasome activity. These data suggest that Y and Z facilitate the ubiquitination of proteins through similar pathways, potentially as E3 ubiquitin ligases, and that the ubiquitination targets the protein for degradation by the proteasome.

We have found further evidence that chronic exposure to low levels of PQ induces oxidative stress in cells and causes a significant decrease in mitochondrial quality. We have also identified two novel proteins, Y and Z, in mediating the oxidative stress response through MAD. Y and Z contribute to protein quality control through MAD by ubiquitination of damaged proteins for targeting to the proteasome for degradation. Even though no sequence homology of these proteins with human proteins was found, it is possible that similar stress response pathways exist in higher mammals, including humans, and further characterization of MAD and its key players may identify novel therapeutic targets for preventative and restorative treatment for those expected to or having been exposed to PQ.

7. Future Directions

Our studies suggest that Y and Z target damaged proteins for degradation by the proteasome by ubiquitination, similar to previously characterized E3 ubiquitin ligases. It would be interesting to test whether these proteins promote MAD by ubiquitinating mitochondrial proteins, specifically. To test this model, wild-type, *Y*Δ, *Z*Δ and *Y*Δ*Z*Δ cells will be treated with and without PQ and MG132, followed by purification of mitochondrial proteins, such as the mitochondrial outer membrane protein that is a previously characterized target of Y [31, 33] – and Aco2p, a highly abundant component of the mitochondrial TCA cycle, whose activity sharply declines under conditions of oxidative stress [47]. In addition, total mitochondrial protein ubiquitination can be measured by performing immunoblotting on mitochondria purified through subcellular fractionation.

We find that deletion of *Y* results in lower mitochondrial redox-state compared to wild-type cells, even in untreated conditions. As the difference between untreated and treated cells is smaller than expected, it is possible that the limit of oxidation that can be measured by mito-roGFP1 has been reached in *Y*Δ cells, such that increased PQ-induced oxidation cannot be measured using this fluorophore. To determine whether this is the case, PQ titration experiments can be carried out in this strain to determine the lower limit of roGFP1. It is also possible that the yeast cell stops cell division when it reaches a certain redox-state of mitochondria, and the lower oxidation limit we observe is the lowest redox-state possible for cell division. To investigate this further we will quantify the redox-state of non-dividing cells and compare with dividing cells.

Redox-state is a good indicator of mitochondrial fitness, but it would be interesting to test mitochondrial quality using a method directly linked to testing functional mitochondrial respiration. This could be done by measuring the membrane potential of mitochondria as increased membrane potential is a direct result of active respiration. The dye DiOC6 is taken up by mitochondria in a membrane potential-dependent manner, and would therefore be appropriate to determine membrane potential.

8. Acknowledgements

Artwork for Figure 2 was performed by Wolfgang Pernice.

I would like to thank my principal investigator, Professor Liza A. Pon, for valuable input throughout this project and for letting me be part of her lab.

I would also like to thank my supervisor Ryo Higuchi-Sanabria for his committed guidance and experimental support. Thanks also to the other members of the Pon laboratory (Elizabeth Stivison, Wolfgang Pernice, Pallavi Srivastava, Istvan Boldogh, Enrique Garcia) for being so welcoming and supportive.

I also wish to thank Professor Leif Bülow for making it possible for me to do my master thesis at Columbia University, and Elisabet Bülow for encouraging me to pursue a career within research.

9. References

[1] R. J. Dinis-Oliveira, J. A. Duarte, A. Sanchez-Navarro, F. Remiao, M. L. Bastos, and F. Carvalho, "Paraquat poisonings: mechanisms of lung toxicity, clinical features, and treatment," *Crit Rev Toxicol,* vol. 38, pp. 13-71, 2008.

[2] R. J. Dinis-Oliveira, F. Remiao, H. Carmo, J. A. Duarte, A. S. Navarro, M. L. Bastos*, et al.*, "Paraquat exposure as an etiological factor of Parkinson's disease," *Neurotoxicology,* vol. 27, pp. 1110-22, Dec 2006.

[3] K. Kuter, P. Nowak, K. Golembiowska, and K. Ossowska, "Increased reactive oxygen species production in the brain after repeated low-dose pesticide paraquat exposure in rats. A comparison with peripheral tissues," *Neurochem Res,* vol. 35, pp. 1121-30, Aug 2010.

[4] A. L. McCormack, M. Thiruchelvam, A. B. Manning-Bog, C. Thiffault, J. W. Langston, D. A. Cory-Slechta*, et al.*, "Environmental risk factors and Parkinson's disease: selective degeneration of nigral dopaminergic neurons caused by the herbicide paraquat," *Neurobiol Dis,* vol. 10, pp. 119-27, Jul 2002.

[5] S. Mostafalou and M. Abdollahi, "Pesticides and human chronic diseases: evidences, mechanisms, and perspectives," *Toxicol Appl Pharmacol,* vol. 268, pp. 157-77, Apr 15 2013.

[6] C. M. Tanner, F. Kamel, G. W. Ross, J. A. Hoppin, S. M. Goldman, M. Korell*, et al.*, "Rotenone, paraquat, and Parkinson's disease," *Environ Health Perspect,* vol. 119, pp. 866-72, Jun 2011.

[7] S. N. Zweig G, Avron M., "Diquat (I,I'-ethylene-2,2'-dipyridylium dibromide) in photo-reactions of isolated chloroplasts," *Biochimica et biophysica acta.,* vol. 109, pp. 332-46, 1965.

[8] H. M. Hassan, "Exacerbation of superoxide radical formation by paraquat," *Methods Enzymol,* vol. 105, pp. 523-32, 1984.

[9] M. Blaszczynski, J. Litwinska, D. Zaborowska, and T. Bilinski, "The role of respiratory chain in paraquat toxicity in yeast," *Acta Microbiol Pol,* vol. 34, pp. 243-54, 1985.

[10] P. R. Castello, D. A. Drechsel, and M. Patel, "Mitochondria are a major source of paraquat-induced reactive oxygen species production in the brain," *J Biol Chem,* vol. 282, pp. 14186-93, May 11 2007.

[11] K. Hirai, H. Witschi, and M. G. Cote, "Mitochondrial injury of pulmonary alveolar epithelial cells in acute paraquat intoxication," *Exp Mol Pathol,* vol. 43, pp. 242-52, Oct 1985.

[12] M. Tomita, "Comparison of one-electron reduction activity against the bipyridylium herbicides, paraquat and diquat, in microsomal and mitochondrial fractions of liver, lung and kidney (in vitro)," *Biochem Pharmacol,* vol. 42, pp. 303-9, Jul 5 1991.

[13] H. M. Cocheme and M. P. Murphy, "Complex I is the major site of mitochondrial superoxide production by paraquat," *J Biol Chem,* vol. 283, pp. 1786-98, Jan 25 2008.

[14] B. Alberts, *Molecular biology of the cell*, Sixth edition. ed. New York, NY: Garland Science, Taylor and Francis Group, 2015.

[15] K. Luce and H. D. Osiewacz, "Increasing organismal healthspan by enhancing mitochondrial protein quality control," *Nat Cell Biol,* vol. 11, pp. 852-8, Jul 2009.

[16] A. M. Nargund, M. W. Pellegrino, C. J. Fiorese, B. M. Baker, and C. M. Haynes, "Mitochondrial import efficiency of ATFS-1 regulates mitochondrial UPR activation," *Science,* vol. 337, pp. 587-90, Aug 3 2012.

[17] A. Weil, K. Luce, S. Drose, I. Wittig, U. Brandt, and H. D. Osiewacz, "Unmasking a temperature-dependent effect of the P. anserina i-AAA protease on aging and development," *Cell Cycle,* vol. 10, pp. 4280-90, Dec 15 2011.

[18] W. Voos, "Chaperone-protease networks in mitochondrial protein homeostasis," *Biochim Biophys Acta,* vol. 1833, pp. 388-99, Feb 2013.

[19] R. J. Youle and A. M. van der Bliek, "Mitochondrial fission, fusion, and stress," *Science,* vol. 337, pp. 1062-5, Aug 31 2012.

[20] A. M. Pickrell and R. J. Youle, "The roles of PINK1, parkin, and mitochondrial fidelity in Parkinson's disease," *Neuron,* vol. 85, pp. 257-73, Jan 21 2015.

[21] K. L. Fehrenbacher, H. C. Yang, A. C. Gay, T. M. Huckaba, and L. A. Pon, "Live cell imaging of mitochondrial movement along actin cables in budding yeast," *Curr Biol,* vol. 14, pp. 1996-2004, Nov 23 2004.
[22] R. Higuchi, J. D. Vevea, T. C. Swayne, R. Chojnowski, V. Hill, I. R. Boldogh*, et al.*, "Actin dynamics affect mitochondrial quality control and aging in budding yeast," *Curr Biol,* vol. 23, pp. 2417-22, Dec 2 2013.
[23] A. Neutzner, R. J. Youle, and M. Karbowski, "Outer mitochondrial membrane protein degradation by the proteasome," *Novartis Found Symp,* vol. 287, pp. 4-14; discussion 14-20, 2007.
[24] E. D. Werner, J. L. Brodsky, and A. A. McCracken, "Proteasome-dependent endoplasmic reticulum-associated protein degradation: an unconventional route to a familiar fate," *Proc Natl Acad Sci U S A,* vol. 93, pp. 13797-801, Nov 26 1996.
[25] N. N. Fang, G. T. Chan, M. Zhu, S. A. Comyn, A. Persaud, R. J. Deshaies*, et al.*, "Rsp5/Nedd4 is the main ubiquitin ligase that targets cytosolic misfolded proteins following heat stress," *Nat Cell Biol,* vol. 16, pp. 1227-37, Dec 2014.
[26] W. K. Huh, J. V. Falvo, L. C. Gerke, A. S. Carroll, R. W. Howson, J. S. Weissman*, et al.*, "Global analysis of protein localization in budding yeast," *Nature,* vol. 425, pp. 686-91, Oct 16 2003.
[27] A. Richardson, R. G. Gardner, and G. Prelich, "Physical and genetic associations of the X ubiquitin ligase with Cdc48 and SUMO," *PLoS One,* vol. 8, p. e76424, 2013.
[28] A. Stein, A. Ruggiano, P. Carvalho, and T. A. Rapoport, "Key steps in ERAD of luminal ER proteins reconstituted with purified components," *Cell,* vol. 158, pp. 1375-88, Sep 11 2014.
[29] A. Sickmann, J. Reinders, Y. Wagner, C. Joppich, R. Zahedi, H. E. Meyer*, et al.*, "The proteome of Saccharomyces cerevisiae mitochondria," *Proc Natl Acad Sci U S A,* vol. 100, pp. 13207-12, Nov 11 2003.
[30] E. E. Patton, A. R. Willems, D. Sa, L. Kuras, D. Thomas, K. L. Craig*, et al.*, "Cdc53 is a scaffold protein for multiple Cdc34/Skp1/F box protein complexes that regulate cell division and methionine biosynthesis in yeast (vol 12, pg 914, 1998)," *Genes & Development,* vol. 12, pp. 3144-3144, Oct 1 1998.
[31] M. M. Cohen, E. A. Amiott, A. R. Day, G. P. Leboucher, E. N. Pryce, M. H. Glickman*, et al.*, "Sequential requirements for the GTPase domain of the mitofusin Fzo1 and the ubiquitin ligase SCFY in mitochondrial outer membrane fusion," *J Cell Sci,* vol. 124, pp. 1403-10, May 1 2011.
[32] D. Finley, H. D. Ulrich, T. Sommer, and P. Kaiser, "The ubiquitin-proteasome system of Saccharomyces cerevisiae," *Genetics,* vol. 192, pp. 319-60, Oct 2012.
[33] M. M. Cohen, G. P. Leboucher, N. Livnat-Levanon, M. H. Glickman, and A. M. Weissman, "Ubiquitin-proteasome-dependent degradation of a mitofusin, a critical regulator of mitochondrial fusion," *Mol Biol Cell,* vol. 19, pp. 2457-64, Jun 2008.
[34] R. D. Gietz, R. H. Schiestl, A. R. Willems, and R. A. Woods, "Studies on the transformation of intact yeast cells by the LiAc/SS-DNA/PEG procedure," *Yeast,* vol. 11, pp. 355-60, Apr 15 1995.
[35] C. Liu, J. Apodaca, L. E. Davis, and H. Rao, "Proteasome inhibition in wild-type yeast Saccharomyces cerevisiae cells," *Biotechniques,* vol. 42, pp. 158, 160, 162, Feb 2007.
[36] I. Boldogh, N. Vojtov, S. Karmon, and L. A. Pon, "Interaction between mitochondria and the actin cytoskeleton in budding yeast requires two integral mitochondrial outer membrane proteins, Mmm1p and Mdm10p," *J Cell Biol,* vol. 141, pp. 1371-81, Jun 15 1998.
[37] C. L. Ladner, J. Yang, R. J. Turner, and R. A. Edwards, "Visible fluorescent detection of proteins in polyacrylamide gels without staining," *Anal Biochem,* vol. 326, pp. 13-20, Mar 1 2004.
[38] J. D. Vevea, D. M. Wolken, T. C. Swayne, A. B. White, and L. A. Pon, "Ratiometric biosensors that measure mitochondrial redox state and ATP in living yeast cells," *J Vis Exp,* 2013.
[39] J. Durieux, S. Wolff, and A. Dillin, "The cell-non-autonomous nature of electron transport chain-mediated longevity," *Cell,* vol. 144, pp. 79-91, Jan 7 2011.

[40] S. Fritz, N. Weinbach, and B. Westermann, "Y is an F-box protein required for maintenance of fusion-competent mitochondria in yeast," *Molecular Biology of the Cell,* vol. 14, pp. 2303-2313, Jun 2003.
[41] T. L. Ulery, S. H. Jang, and J. A. Jaehning, "Glucose repression of yeast mitochondrial transcription: kinetics of derepression and role of nuclear genes," *Mol Cell Biol,* vol. 14, pp. 1160-70, Feb 1994.
[42] L. N. Dimitrov, R. B. Brem, L. Kruglyak, and D. E. Gottschling, "Polymorphisms in multiple genes contribute to the spontaneous mitochondrial genome instability of Saccharomyces cerevisiae S288C strains," *Genetics,* vol. 183, pp. 365-83, Sep 2009.
[43] M. A. Lebedeva and G. S. Shadel, "Cell cycle- and ribonucleotide reductase-driven changes in mtDNA copy number influence mtDNA Inheritance without compromising mitochondrial gene expression," *Cell Cycle,* vol. 6, pp. 2048-57, Aug 15 2007.
[44] J. R. McFaline-Figueroa, J. Vevea, T. C. Swayne, C. Zhou, C. Liu, G. Leung*, et al.*, "Mitochondrial quality control during inheritance is associated with lifespan and mother-daughter age asymmetry in budding yeast," *Aging Cell,* vol. 10, pp. 885-95, Oct 2011.
[45] G. T. Hanson, R. Aggeler, D. Oglesbee, M. Cannon, R. A. Capaldi, R. Y. Tsien*, et al.*, "Investigating mitochondrial redox potential with redox-sensitive green fluorescent protein indicators," *J Biol Chem,* vol. 279, pp. 13044-53, Mar 26 2004.
[46] A. Ruggiano, O. Foresti, and P. Carvalho, "Quality control: ER-associated degradation: protein quality control and beyond," *J Cell Biol,* vol. 204, pp. 869-79, Mar 17 2014.
[47] L. J. Yan, R. L. Levine, and R. S. Sohal, "Oxidative damage during aging targets mitochondrial aconitase," *Proc Natl Acad Sci U S A,* vol. 94, pp. 11168-72, Oct 14 1997.

10. Supplemental information

Supplemental Table 1. Sequences of proteins used in this study

Protein	Protein Sequence
X	XXXXXXXXXXXXXXXXXXXXXXXXXXXXXXXXXXXXXXXXXXXXXXXXXXXXXXXXXXXXXXX XXXXXXXXXXXXXXXXXXXXXXXXXXXXXXXXXXXXXXXXXXXXXXXXXXXXXXXXXXXXXXX XXXXXXXXXXXXXXXXXXXXXXXXXXXXXXXXXXXXXXXXXXXX
Y	YYYYYYYYYYYYYYYYYYYYYYYYYYYYYYYYYYYYYYYYYYYYYYYYYYYYYYYYYYYYYYY YYYYYYYYYYYYYYYYYYYYYYYYYYYYYYYYYYYYYYYYYYYYYYYYYYYYYYYYYYYYYYY YYYYYYYYYYYYYYYYYYYYYYYYYYYYYYYYYYYYYYYYYYYYYYYYYYYYYYYYYYYYYYY YYYYYYYYYYYYYYYYYYYYYYYYYYYYYYYYYYYYYYYYYYYYYYYYYYYYYYYYYYYYYYY YYYYYYYYYYYYYYYYYYYYYYYYYYYYYYYYYYYYYYYYYYYYYYYYYYYYYYYYYYYYYYY YYYYYYYYYYYYYYYYYYYYYYYYYYYYYYYYYYYYYYYYYYYYYYYYYYYYYYYYYYYYYYY YYYYYYYYYYYYYYYYYYYYYYYYYYYYYYYYYYYYYYYYYYYYYYYYYYYYYYYYYYYYYYY YYYYYYYYYYYYYYYYYYYYYYYYYYYYYYYYYYYYYYYYYYYYYYYYYYYYYYYYYYYYYYY YYYYYYYYYYYYYYYYYYYYYYYYYYYYYYYYYYYYYYYYYYYYYYYYYYYYYYYYYYYYYYY YYYYYYYYYYYYYYYYYYYYYYYYYYYYYY
Z	ZZZZZZZZZZZZZZZZZZZZZZZZZZZZZZZZZZZZZZZZZZZZZZZZZZZZZZZZZZZZZZZ ZZZZZZZZZZZZZZZZZZZZZZZZZZZZZZZZZZZZZZZZZZZZZZZZZZZZZZZZZZZZZZZ ZZZZZZZZZZZZZZZZZZZZZZZZZZZZZZZZZZZZZZZZZZZZZZZZZZZZZZZZZZZZZZZ ZZZZZZZZZZZZZZZZZZZZZZZZZZZZZZZZZZZZZZZZZZZZZZZZZZZZZZZZZZZZZZZ ZZZZZZZZZZZZZZZZZZZZZZZZZZZZZZZZZZZZZZZZZZZZZZZZZZZZZZZZZZZZZZZ ZZZZZZZZZZZZZZZZZZZZZZZZZZZZZZZZZZZZZZZZZZZZZZZZZZZZZZZZZZZZZZZ ZZZZZZZZZZZZZZZZZZZZZZZZZZZZZZZZZZZZZZZZZZZZZZZZZZZZZZZZZZZZZZZ ZZZZZZZZZZZZZZZZZZZZZZZZZZZZZZZZZZZZZZZZZZZZZZZZZZZZZZZZZZZZZZZ ZZZZZZZZZZZZZZZZZZZZZZZZZZZZZZZZZZZZZZZZZZZZZZZZZZZZZZZZZZZZZZZ ZZZZZZZZZZZZZZZZZZZZZZZZZZZZZZZZZZZZZZZZZZZZZZZZZZZZZZZZZZZZZZZ ZZZZZZZZZZZZZZZZZZZZZZZZZZZZZZZZZZZZZZZZZZZZZZZZZZZZZZZZZZZZZZZ ZZZZZZZZZZZZZZZZZZZZZZZZZZZZZZZZZZZZZZZZZZZZZZZZZZZZZZZZZZZZZZZ ZZZZZZZZZZZZZZZZZZZZZZZZZZZZZZZZZZZZZZZZZZZZZZZZZZZ

Supplemental Table 2. Strains used in this study

Strains	Genotype	Source
BY4741	*MATa his3Δ1 leu2Δ0 met15Δ0 ura3Δ0*	Open Biosystems
MLY002	*MATa his3Δ1 leu2Δ0 met15Δ0 ura3Δ0 ZΔ::LEU2*	This study
MLY003	*MATa his3Δ1 leu2Δ0 met15Δ0 ura3Δ0* [pmito-roGFP1:*URA3*]	This study
MLY004	*MATa his3Δ1 leu2Δ0 met15Δ0 ura3Δ0 YΔ::LEU2*	This study
MLY005	*MATa his3Δ1 leu2Δ0 met15Δ0 ura3Δ0 XΔ::LEU2*	This study
MLY006	*MATa his3Δ1 leu2Δ0 met15Δ0 ura3Δ0 ZΔ::LEU2* [pmito-roGFP1:*URA3*]	This study
MLY007	*MATa his3Δ1 leu2Δ0 met15Δ0 ura3Δ0 XΔ::LEU2* [pmito-roGFP1:*URA3*]	This study
MLY009	*MATa his3Δ1 leu2Δ0 met15Δ0 ura3Δ0 YΔ::LEU2* [pmito-roGFP1:*URA3*]	This study
MLY010	*MATa his3Δ1 leu2Δ0 met15Δ0 ura3Δ0 XΔ::LEU2 CIT1-GFP(S65T)-HIS3*	This study
MLY011	*MATa his3Δ1 leu2Δ0 met15Δ0 ura3Δ0 YΔ::LEU2 CIT1-GFP(S65T)-HIS3*	This study
MLY012	*MATa his3Δ1 leu2Δ0 met15Δ0 ura3Δ0 ZΔ::LEU2 CIT1-GFP(S65T)-HIS3*	This study
MLY015	*MATa his3Δ1 leu2Δ0 met15Δ0 ura3Δ0 YΔ::LEU2 ZΔ::URA3 CIT1-GFP(S65T)-HIS3*	This study
MLY016	*MATa his3Δ1 leu2Δ0 met15Δ0 ura3Δ0 YΔ::LEU2 ZΔ::kanMX-6*	This study
MLY017	*MATa his3Δ1 leu2Δ0 met15Δ0 ura3Δ0 YΔ::LEU2 ZΔ::kanMX-6* [pmito-roGFP1:*URA3*]	This study
RHY116	*MATa his3Δ1 leu2Δ0 met15Δ0 ura3Δ0 CIT1-GFP(S65T)-HIS3*	[22]

Supplemental Table 3. Primers used in this study

Purpose	Forward Primer	Reverse Primer	Forward Screening Primer	Reverse Screening Primer
X*Δ *LEU2	AGGAATGAACTCCAG GAAAGGCCAACTTATT CGACGGTAATGCAGG TCGACAACCCTTAAT	ATTTTAATATATTAGT GTCTGGTTTAAAAGTC ATACTTCTGCAGCGTA CGGATATCACCTA	GTGAGCTCGAA ATGACGAACCA GTC	AGCACTCTTC TTCAGATGTC AGACAACG
Y*Δ *LEU2	ACAATTTTTCGGTATT AGTTACTAAAAGGCTC ACATATACTGCAGGT CGACAACCCTTAAT	TGTGTCAGGATGCTA CTTTTGGAAACCTCCT TAAATATGAGCAGCG TACGGATATCACCTA	GCACGTTTCCG GTAAAATCTTG GG	CGTGGTACCC AGGTCGATAC C
Z*Δ *LEU2	ATTAGAAACAATAGGA AACAACAGAGTCGGA AGAAGCCAATGCAGG TCGACAACCCTTAAT	CGAGAGCGGAGGAA GGGTAAGGAAGTAAA GAGAAAAATATGCAG CGTACGGATATCACC TA	CATCTGATGAA GTAGTGATCCG ACAATTC	GGGAAGGGA ATTTGCTGCA ATC
Z*Δ *kanMX-6	ATTAGAAACAATAGGA AACAACAGAGTCGGA AGAAGCCAACGGATC CCCGGGTTAATTAA	CGAGAGCGGAGGAA GGGTAAGGAAGTAAA GAGAAAAATATGAATT CGAGCTCGTTTAAAC	CATCTGATGAA GTAGTGATCCG ACAATTC	GGGAAGGGA ATTTGCTGCA ATC
CIT1-GFP	AAAATACAAGGAGTT GGTAAAGAAAATCGA AAGTAAGAACCGGAT CCCCGGGTTAATTAA	AATAGTCGCATACCCT GAATCAAAAATCAAAT TTTCCTTAGAATTCGA GCTCGTTTAAAC		